19

Numerical Simulation of Radiolysis Gas Detonations in a BWR Exhaust Pipe and Mechanical Response of the Piping to the Detonation Pressure Loads

Mike Kuznetsov, Alexander Lelyakin and Wolfgang Breitung
Institute for Nuclear and Energy Technologies, Karlsruhe Institute of Technology
Germany

1. Introduction

Radiolysis gas ($2H_2+O_2$) can accumulate in steam piping of Boiling Water Nuclear Reactor (BWR) in case of steam condensation. A detonation of radiolysis gas was the likeliest cause of the pipe ruptures in the Hamaoka-1 and Brunsbüttel accidents (Nakagami, 2002; Schulz et al., 2002). In both cases the failed pipes were initially under the operating pressure of 70 bar. During the detonation accident the pressure rose up to 1000 bar or more. In the current paper we consider a typical BWR exhaust pipe and first evaluate the maximum pressure load in case of a radiolysis gas detonation at an initial pressure of 1.6 bar and a temperature of 35 °C. Next, the mechanical response of the exhaust pipe and its possible damage will be numerically evaluated.

The typical exhaust pipe investigated in this study is shown in Fig. 1. It consists of two parts with an outer diameter of 510 and 419 mm fabricated from stainless steel DIN 1.4541. In reality, the exhaust pipe is filled with nitrogen initially. Radiolysis gas (RG) with steam can enter through an exhaust valve due to an opening procedure or due to a leak. In case of a slow long time steam condensation, the radiolysis gas can accumulate at the top of the exhaust pipe. Thus, without an additional ventilation, the "worst case" atmosphere in the exhaust pipe has an initial pressure of 1.6 bar (controlled by the 6 m height of the water level) and consists of radiolysis gas diluted with nitrogen.

According to the recommendations of the Reactor Safety Commission (Germany) for radiolysis gas control in BWR plants it is demanded to determine the reaction pressure for the highest radiolysis gas concentration which could arise. Our previous data analysis (Kuznetsov et al., 2007a) was based on the postulated detonation of pure radiolysis gas, consisting of a stoichiometric hydrogen-oxygen mixture, as the "worst case" scenario. In this study three levels of pressure loads for "worst case" conditions were evaluated in these works: (1) the stationary detonation pressure of about 29 bar; (2) the local deflagration-to-detonation transition (DDT) pressure of 62.5 bar; and (3) the reflected Chapman-Jouguet (CJ) pressure of 71 bar as the maximum detonation pressure that occurs at the tube end. The characteristic pressure loading time was estimated to be about 2 ms, which corresponds to the quasi-static loading regime for a tube of 510 mm outer diameter and 15 mm of wall

thickness (the weakest tube part). It was demonstrated that the reflected detonation wave at the end of the exhaust pipe causes a maximum circumferential strain of 0.11%. Normal detonation at the main part of the exhaust pipe causes a strain of about 0.045%. This means that "worst-case" scenario of radiolysis gas detonation would not lead to the structural damage of such pipe.

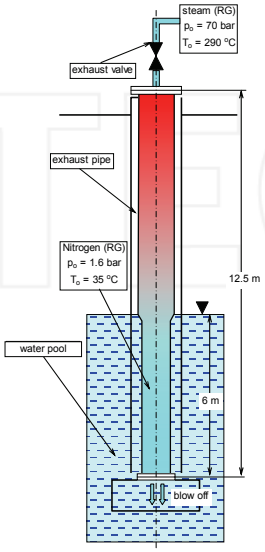

Fig. 1. Schematic of typical BWR exhaust pipe: radiolysis gas (RG) coloured in red

Detailed analysis of experiments (Kuznetsov et al., 2002; Schröder et al., 2006; Kuznetsov et al., 2007b) with radiolysis gas detonations in closed pipes showed that much higher maximum detonation pressures than the reflected pressure and the DDT pressure could occur in reality. The main purpose of this work is to find out the real "worst case" scenario in order to evaluate the integrity of a BWR exhaust pipe using a 1D numerical code for deflagration-to-detonation simulation (FA1D). These data are required for BWR safety analysis and future design guidelines for BWRs.

2. Experimental analysis of radiolysis gas detonations

In (Kuznetsov et al., 2007a) stoichiometric H_2-O_2 mixtures were examined as a "worst case" scenario, because they have the highest energy density and thus the largest potential for pipe deformations. Radiolysis gas mixtures with arbitrary nitrogen dilutions have also been discussed in this work. According to the references (Schröder et al., 2006; Kuznetsov et al., 2007a) the principal sequence of a radiolysis gas combustion, schematically represented in Fig. 2, changes with growing nitrogen dilutions as follows:

- after weak ignition of the gas at x = 0 a slower flame acceleration takes place compared to pure radiolysis gas;
- due to the longer foregoing deflagration process the DDT point shifts to the tube end;
- the precursor shock wave ahead of the flame has a smaller Mach number and thus a lower pressure amplitude;

- the DDT peak pressure increases on the one hand because of increasing pre-compression; on the other hand the theoretical CJ-pressure drops because of the nitrogen dilution;
- because of the longer run-up-distance to the DDT point the time gap between detonation onset and reflection decreases; this leads to the actual worst case situation when both processes overlap and the detonation is initiated at the pressure of the reflected precursor shock wave.

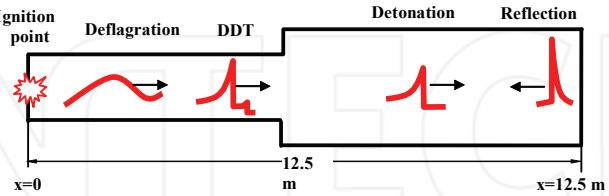

Fig. 2. Principal sequence of the combustion process in a BWR exhaust pipe with nitrogen diluted radiolysis gas

Thus, with increasing nitrogen dilution the DDT point shifts towards the tube end resulting in extremely high pressures as result of cumulative effects of pre-compression, reflection and local explosion during the DDT process itself. Because of smaller amount of remaining unburned material during the DDT process the resulting peak pressure from DDT and reflection will be shorten and the characteristic pressure load time will decrease. However reduced duration of a pressure load can cause a smaller dynamic load factor and less strain in a loaded tube (Kuznetsov et al., 2007b).
The total effect of nitrogen dilution on the maximum dynamic piping stress and strain cannot be evaluated without detailed numerical simulations, because of the co-existence of several gas dynamic effects. In this work therefore the influence of nitrogen dilution will be quantitatively determined by systematic numeric simulation of the radiolysis gas combustion sequence depicted in Fig. 2. The goal of the calculations is the evaluation of maximum pressures that can occur for the deflagration/detonation of $2H_2+O_2+xN_2$ mixtures in an exhaust pipe. In a second step, the structural dynamic response of the exhaust pipe to the calculated dynamic pressure loads will be examined.

3. FA1D code description

3.1 The model

For the numerical simulation of reacting flow problems a CFD "in house" code was developed. In order to simplify the program and to make it more quick and flexible, the program was based on the following assumptions:

- solution of the reactive Euler equations, i.e. neglect of molecular transportation processes such as diffusion, thermal conduction and viscosity;
- no turbulence;
- 1-dimensional geometry, i.e. neglect of real tube geometry (variable cross-section), radial gradients of concentrations, pressure, temperature and fluid velocity;
- one global dominant reaction for the H_2/O_2-combustion;
- prescribed flame acceleration law;
- temperature-dependent thermodynamic data for all components (H_2, O_2, H_2O, N_2);

- 1st order solution procedure, numerical cell size in the present problem is 1-2 mm;
- adiabatic assumption (no heat losses of gas to tube wall);
- ideally reflecting boundary conditions at the tube ends.

In particular the last assumption leads to conservative results during the pressure computation. The model is based on the following 1D Euler equations:

$$\frac{\partial \rho}{\partial t} + \frac{\partial \rho u}{\partial x} = 0 \tag{1}$$

$$\frac{\partial \rho u}{\partial t} + \frac{\partial \rho u^2}{\partial x} + \frac{\partial p}{\partial x} = 0 \tag{2}$$

$$\frac{\partial E}{\partial t} + \frac{\partial u(E+p)}{\partial x} = -\sum r_i \cdot H_i^f \cdot Q \tag{3}$$

$$\frac{\partial \rho f_i}{\partial t} + \frac{\partial \rho u f_i}{\partial x} = \mu_i \cdot r_i \cdot Q \tag{4}$$

Here ρ - density, u - velocity, E - total energy per unit volume (kinetic+thermal), f_i - mass fraction of components, Q - reaction rate, r_i - stoichiometric coefficients (negative for reagents, positive for products), H_i^f - enthalpy of formation, μ_i - molecular mass. Simulation of flame propagation is based on flame position tracking. Flame position is calculated as:

$$\frac{dX_{fp}}{dt} = u\left(X_{fp}(t), t\right) + FV\left(X_{fp}(t)\right) \tag{5}$$

Here $FV(x)$ is a prescribed flame acceleration profile. To simulate a detonation, $FV(x)$ can be set equal to the sound speed of burned gas. So, the reaction rate is calculated as follows:

$$Q = \begin{cases} Q_0 \cdot \dfrac{\rho f_l}{\mu_l} & x < X_{fp} \\ 0 & x > X_{fp} \end{cases} \tag{6}$$

Here l is the index of the limiting reagent (in our calculations - H_2). The choice of Q_0 is not very important. Its value determines only the width of the reaction zone. It should be sufficiently high, to make this zone narrow, but not very high to not disturb the numerical stability of the model. If we consider the computational cell where the flame front is, we will see that $Q_0 = \dfrac{FV}{\Delta x}$ is a reasonable choice for the reaction rate.

However, such a simple model of combustion will result always in complete combustion of the reagents. The real equilibrium state after the combustion consists not only of products, but also of unreacted reagents and radicals representing intermediate stages of the combustion. The completeness of the combustion is determined mostly by the temperature but also by pressure and initial concentrations of species. To determine the completeness of the combustion it is necessary to consider reverse reactions together with the forward ones. The ratio of rates of forward and reverse reactions is determined by:

$$\frac{Q_f}{Q_r} = K = \left(\frac{P_{atm}}{RT}\right)^{\sum r_i} \cdot \exp\left(\sum r_i \cdot \left(\frac{S_i}{R} - \frac{H_i}{RT}\right)\right) \cdot \prod\left(\frac{\rho f_i}{\mu_i}\right)^{-r_i} \tag{7}$$

where S_i and H_i are molar entropy and enthalpy of species, respectively. The net reaction rate is then

$$Q = Q_f - Q_r = Q_f \cdot \left(1 - \frac{1}{K}\right) \tag{8}$$

So we can see that a correction factor has to be introduced to the reaction rate, which is determined by the thermodynamic properties of the mixture. It is not necessary to follow this formula exactly as long as we don't investigate detailed chemistry with exact reaction rates. The only important thing here is the sign of the net reaction rate and equilibrium point where $K = 1$ and $Q = 0$. We found that the following approximate formula gives the same result as as the exact one, Eq. (8):

$$Q = Q_f \cdot \begin{cases} 1 & \ln K > 1 \\ \ln K & -1 < \ln K < 1 \\ -1 & \ln K < -1 \end{cases} \tag{9}$$

The advantage of this formula is the possibility to avoid an exponentiation at every cell in every time step. Another advantage is that the correction factor applied to the reaction rate is less than one by absolute value, so such a correction will not influence the numerical stability of calculations.

3.2 Flame acceleration model and code validation

An important part of the model is the simulation of the flame acceleration after the first weak ignition. This phase determines amplitude and length of the pre-compressed zone, which is formed ahead of the flame front in the unburned gas. The pressure amplitude depends particularly on the effective maximum burning velocity S_{max} of the turbulent flame developing in the pipe. Since the FA1D-code does not have any turbulence model, three radiolysis gas experiments in smooth pipes (Kuznetsov et al., 2002; Kuznetsov et al., 2005; Liberman et al., 2009) with different gas mixtures have been analyzed, to evaluate the effective burning speed S_{max} and the flame acceleration law.

Experimental data analysis showed that S_{max} normalized by the fundamental laminar flame speed S_L which lies in the range of S_L = 4 - 12 m/s, practically doesn't change and has an average value of S_{max}/S_L = 17.5. This value is also consistent with general correlations for the turbulent burning speed S_T for different gases at high degree of turbulence which gives S_T/S_L values up to 17 (Bradley, 1992). Therefore the use of a maximum turbulent burning speed of $S_{max} = 17.5 \cdot S_L$ for the examined radiolysis gas - nitrogen mixtures, seems to be a reasonable number for extrapolation to all diluted radiolysis gas mixtures in the present work. The laminar flame speed S_L for mixtures with unknown fundamental flame velocity was computed using the Cantera code with a verified planar flame model (Goodwin, 2001) and a detailed H/O/N reaction mechanism (Lutz, 1988).

A detailed sensitivity study showed that not only the maximum burning speed S_{max}, but also the flame acceleration from S_0 up to S_{max} can affect the pressure in a pipe before and

after the DDT process. Figure 3 shows a simplified linear approximation of the flame speed evolution in a pipe used in Eq. (5) as the flame acceleration law along the tube. In good agreement with our experimental data (Liberman et al., 2009) a linear flame acceleration law against distance in smooth channels corresponds to the case when the visible flame velocity is proportional to the flame area, which is for so called "finger" flames proportional to the distance along the tube, $S(x) \sim k \cdot x$. This leads to the exponential flame acceleration law against time as follows:

$$S(t) = S_0 \exp(k \cdot t) \tag{10}$$

where $k = \sigma \cdot S_L / R$ is the exponential factor depending on the expansion ratio $\sigma = \rho_u / \rho_b$ of unburned and burned components and tube radius R; $S_0 = S_L$ is the effective initial flame speed. So, with a smaller tube size and a higher mixture reactivity the flame accelerates faster.

For the general description of the deflagration, three main parameters are necessary: the initial flame speed S_0, the flame acceleration distance x_a which depends on the exponential factor k (Eq. (10) and the maximum flame speed S_{max}. At the postulated DDT point x_D the flame speed is increased suddenly to the speed of sound in the burned gas C_p, which can be determined from thermodynamic calculations. This flame speed corresponds to the CJ-detonation.

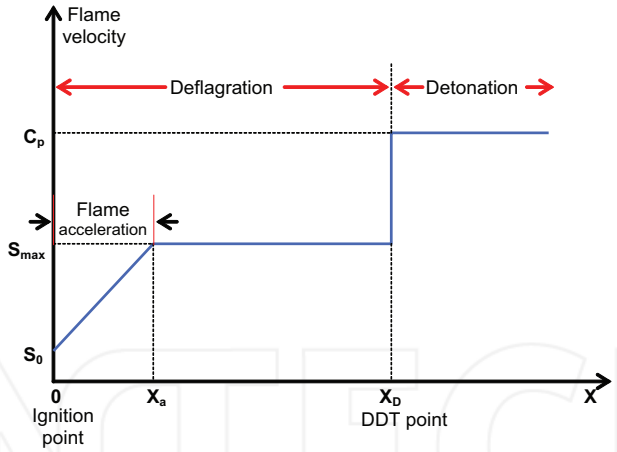

Fig. 3. Dynamics of the flame velocity in the 1D numerical model for DDT in radiolysis gas - nitrogen mixtures

The effects of the two free parameters S_0 and x_a on the peak pressures were examined to be used in detailed model for the flame speed calculations. The flame model used here supplies conservative over-pressure before and after the DDT process.

The numerical model of FA1D was examined in a wide range of initial conditions for detonation experiments with radiolysis gas mixtures (Kuznetsov et al., 2002; Kuznetsov et al., 2005): tube lengths from 3 to 6 m; initial pressures from 0.7 to 10 bar; initial temperatures from 300K to 570K; without and with different inert gases as steam and nitrogen. The experimental validation of the code is required to adjust the three main parameters of the

flame acceleration: the initial burning speed S_0, the flame acceleration distance x_a and the maximum burning speed S_{max}, using experimentally determined trajectories for shock wave and flame front. The DDT point in the calculations was specified at the same distance as observed in the experiments.

Figure 4 shows one example for a comparison of experimental and calculated x-t diagrams for radiolysis gas detonation experiments with 40% H_2O at 10 bar and 570K, with the DDT point x_D at 2 m. Such diagrams represent an array of pressure and light sensor records vs. time at the x position along the tube. According to the previous correlation a maximum burning speed S_{max} = 150 m/s was assumed, an initial speed S_0 = 50 m/s and an acceleration distance x_a = 0.5 m were used in the calculations. The variable pressure scale is indicated by the tick at the right side for each pressure gauge position. In Fig. 4 measured and computed pressure and light signals are depicted. The experimental x-t diagram (Fig. 4, left) shows that behind the leading shock wave (SW) the radiolysis gas mixture is pre-compressed up to 15 bar compared to 10 bar of initial pressure. The calculations give a somewhat stronger leading shock wave with a pressure of 21 bar.

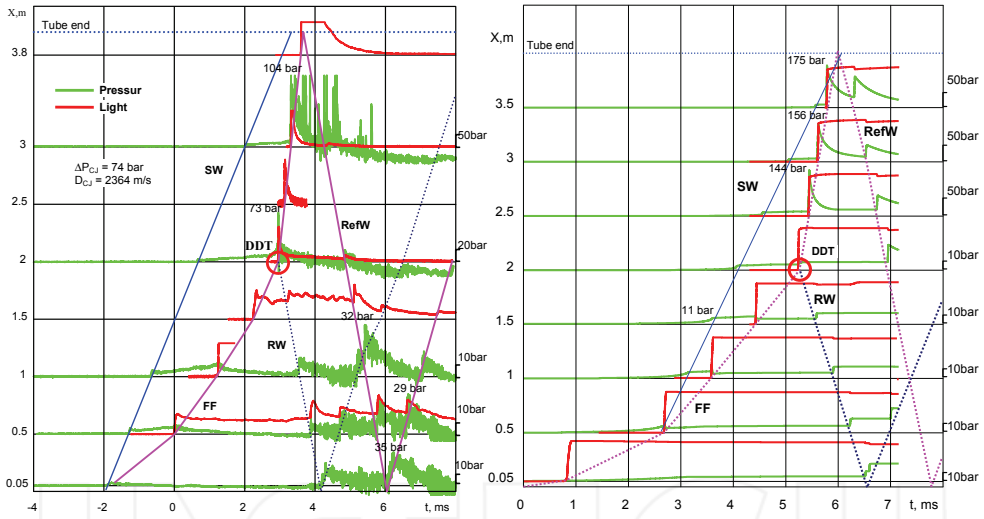

Fig. 4. Detonation experiment (left) and 1D numerical simulation (right) for a radiolysis gas mixture with 40% steam (p_0 =10 bar, T_0 =300°C). Plotted lines: SW = shock wave; FF = flame front; RW = retonation wave; RefW = reflection wave

Generally, the measurements and calculations show good agreement of pressure and light signals and shock wave trajectories. The test calculations and further comparisons with experiments, will show that the developed 1D program is able to reproduce all necessary dynamic pressure effects and that it can be used for the prediction of real pressure loads.

4. Structural dynamics response

For the computation of a pipe widening under a certain internal pressure the motion equation for a thin infinite expanded cylinder (Fig. 5) was solved. The tube with an outer

radius R and wall thickness h exposed to an isotropic internal overpressure $p(t)$ experiences a deformation $x(t)$. To calculate the tube response at the different regimes of internal pressure loads the following assumptions are introduced: a) cylindrical symmetry; b) linear Hooke's law for deformations (linear elastic oscillator).

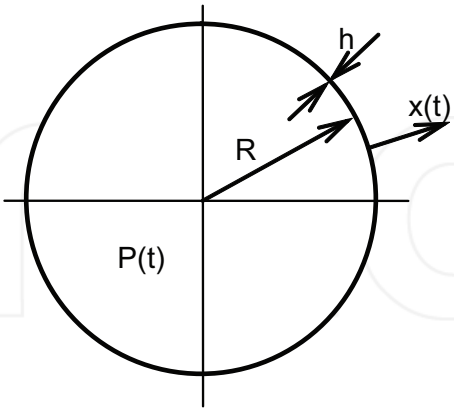

Fig. 5. Tube parameters

The following differential equation describes the structural response of a long pipe in the linear elastic approach:

$$\frac{\partial^2}{\partial t^2}x(t)+\mu\frac{\partial}{\partial t}x(t)+\Omega^2 x(t)=\frac{p(t)}{\rho\cdot h} \tag{11}$$

$$\Omega=\sqrt{\frac{E}{\rho\cdot(1-\nu^2)\cdot R^2}} \tag{12}$$

where Ω is the circular frequency of the tube; ν is the Poisson's ratio; μ is the damping factor; E is the Young's modulus of elasticity; ρ is the density; $x(t)$ is the wall displacement. In terms of engineering strain $\varepsilon = x/R$, the following differential equation governs the structural response of a pipe:

$$\frac{\partial^2}{\partial t^2}\varepsilon(t)+\mu\frac{\partial}{\partial t}\varepsilon(t)+\Omega^2\varepsilon(t)=\frac{p(t)}{\rho\cdot R\cdot h} \tag{13}$$

Of course, the model does not describe the behavior of a finite cylindrical shell like a tube with flanges. The time dependent pressure function $p(t)$ might be described as an analytical function or as an output file of the pressure-time history from FA1D simulations. It also could be a measured pressure-time dependency obtained by pressure sensors. For simple pressure function $p(t)$ equation (13) can be solved analytically. For complex pressure functions $p(t)$ the differential equation (13) was solved numerically with a Runge-Kutta method.

Static pressure load. In the simplest case, the pressure does not depend on time $p(t) = P_m$ = const. In this case the maximum tube response is

$$\varepsilon_m = \frac{P_m}{\rho \cdot R \cdot h \cdot \Omega^2} \tag{14}$$

Substitution of Ω from Eq. (11) then gives for the maximum tube response

$$\varepsilon_m = \frac{R \cdot P_m}{E \cdot h} \tag{15}$$

which does not depend on the time (Fig. 6, left). The maximum displacement ε_m = 0.0025 was calculated for stainless steel tube with the following properties as an example:

- Density	ρ = 8000 kg/m³	- Wall thickness	h = 2 mm
- Young's modulus	E = 200000 MPa	- Circular frequency	Ω = 200 kHz
- Outer radius	R = 25 mm	- Maximum overpressure	P_m = 40 MPa

Formula (15) is often used to calculate the maximum design pressure of a tube under static pressure load. However, in the case of a detonation load, the pressure load is highly transient and propagates at high speed. In this case the static design pressure formula (15) gives a value for the maximum displacement that is too low. Let us consider why.

Dynamic response. The dynamic pressure response of the tube (Fig. 5) in simplified form with a damping factor of μ = 0 yields:

$$\frac{\partial^2}{\partial t^2}\varepsilon(t) + \Omega^2 \varepsilon(t) = \frac{p(t)}{\rho \cdot R \cdot h} \tag{16}$$

As an intermediate case from static to dynamic load a quasi-static pressure function can be considered, which is given by

$$p(t) = \begin{cases} 0 & t \le 0 \\ P_m & t > 0 \end{cases} \tag{17}$$

The response of the tube can be calculated analytically as follows

$$\varepsilon(t) = \begin{cases} 0 & t \le 0 \\ \varepsilon_m \cdot \left(1 - \cos(\Omega \cdot t)\right) & t > 0 \end{cases} \tag{18}$$

where ε_m is the static tube response given by Eq. (15). It follows from Eq. (18) that the maximum displacement under quasi-static loading is two times higher than in the static case:

$$\varepsilon(t)_{\max} = 2 \cdot \varepsilon_m = K \cdot \frac{R \cdot p_m}{E \cdot h} \tag{19}$$

So, an amplification factor of K = 2 is determined for a displacement under quasi-static load compared to the static pressure loads. The analytical solution of equation (3) for the simplest step-wise pressure function $p(t)$ = P_m = const (t > 0) is given in Fig. 6 (right). It really shows that the mechanical response of the tube (25 mm i.d., 2 mm wall thickness) to the dynamic

pressure load even in case of the same maximum pressure as for static load ($p(t) = P_m$) can be two times higher.

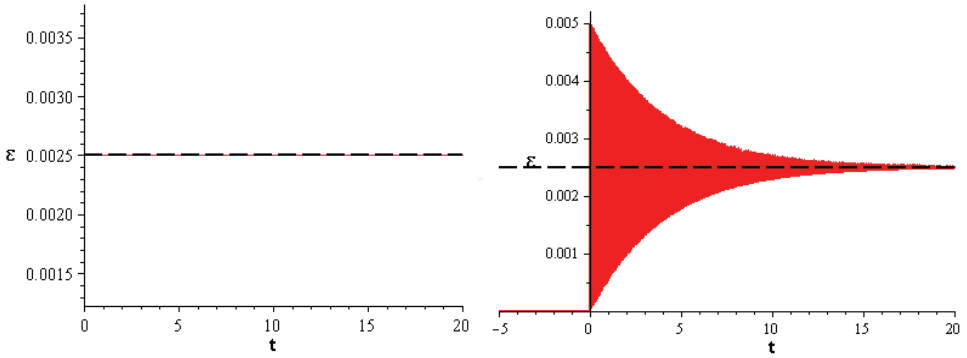

Fig. 6. Static (left) and quasi-static (right) tube responses

In accordance with Baker's (1983) overview, the amplification factor K depends on the value of the product $\Omega \cdot T$, where T is the characteristic time of dynamic loading. For a detonation process, three different pressure profiles with characteristic time T, when $\Omega \cdot T > 40$, can be considered to be analytically derived for the appropriate piping deformation (see Fig. 7): rectangular (I), triangular (II) and exponential function (III), which is the most typical for detonation processes.

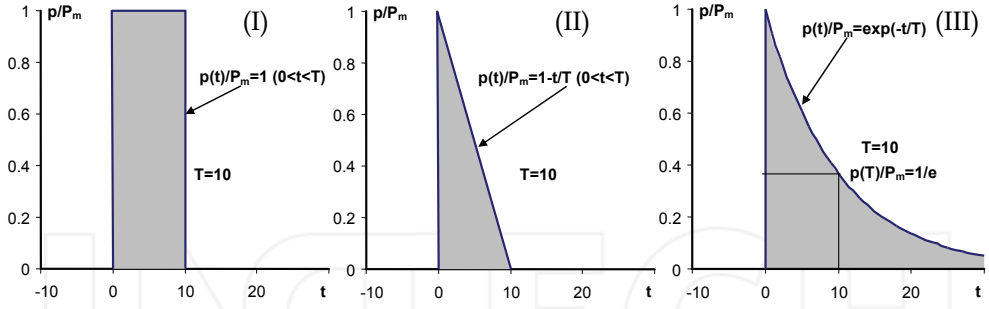

Fig. 7. Typical dynamic pressure functions $p(t)$ used in eq. (16)

The same initial conditions as above for the stainless steel tube were used for the mechanical response calculations. The analytical solutions of equation (13) for these three cases with a damping factor of $\mu = 0.5$ and characteristic time of the pressure load $T = 10$ ms ($\Omega \cdot T > 40$) are given in graphical form in Fig. 8. It was shown that the maximum displacement, which is equal to $\varepsilon_m = 0.005$, for all cases is independent of the shape of the pressure impulse and only proportional to the maximum pressure P_m. In comparison with a static pressure load, where $\varepsilon_m = 0.0025$, this means that the dynamic amplification factor is $K = 2$ for maximum displacement, which is two times larger than for the static case, similar to that for quasi-static pressure loading regime when $\Omega \cdot T > 40$.

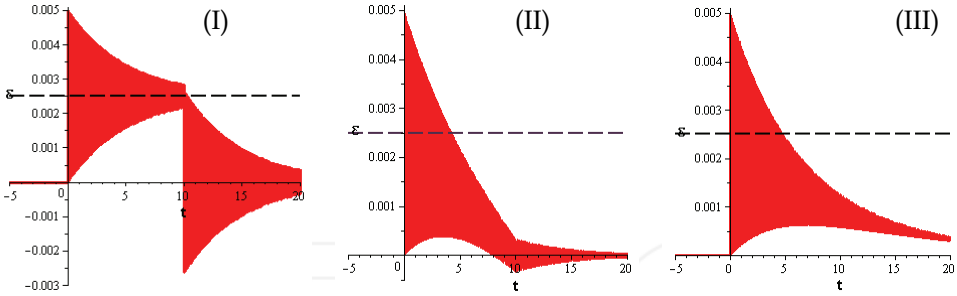

Fig. 8. Calculated tube response to the dynamic load in the quasi-static regime ($\Omega \cdot T > 40$)

In agreement with Baker (1983), it also was shown that in case of impulsive loads for T=0.1 ms, when $\Omega \cdot T < 0.4$, the maximum displacement ε_m of the tube under internal dynamic pressure load is proportional to the pressure impulse $I = \int p(t)dt$, independent of the shape of the pressure function $p(t)$. This explains why the smallest displacement was calculated for a triangular pressure impulse, which has the smallest pressure impulse of all three cases (Fig. 9). The corresponding ratio of the pressure impulses for three cases: $I_I : I_{II} : I_{III} = P_m \cdot T : P_m \cdot T/2 : P_m \cdot T\ (1\text{-}1/e) = 2 : 1 : 1.3$ is the same as that for the calculated maximum displacements: $\varepsilon_I : \varepsilon_{II} : \varepsilon_{III} : = 2 : 1 : 1.3$. In the intermediate case of $0.4 < \Omega \cdot T < 40$, a transient regime will occur with an amplification factor in the range of $0 < K < 2$.

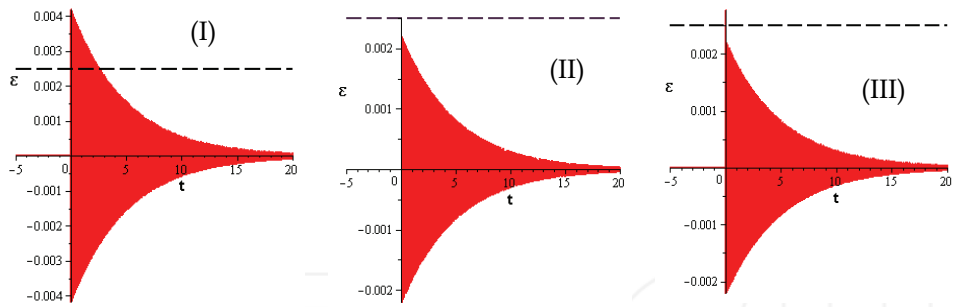

Fig. 9. Tube response to the pressure load in dynamic or impulsive regime ($\Omega \cdot T < 0.4$)

In the present work the time-dependent pressure load function $p(t)$ in equation (13) was also taken from the gas dynamics code FA1D. For such a complex pressure function the differential equation (13) was solved numerically with a Runge-Kutta method. The numerically computed piping strain agreed with the analytical results for the above described simple cases.

Figure 10 shows an example for the calculated mechanical response to a pressure load with a highly resolved pressure function that includes the von Neumann spike, compared to that without von Neumann spike (low time resolution >10 μs). This example demonstrates that the very narrow von Neumann spike has practically no effect on the resulting pipe strain. Under detonation pressure load the maximum displacement ε_m is mainly determined by the Chapman-Jouguet pressure p_{CJ} which is the effective detonation pressure. Using equation

(13) with an amplification factor K = 2 for p_m = 85 bar, the maximum displacement ε_m = 0.14% is very close to the calculated value of 0.12% obtained using the measured pressure $p(t)$ and a Runge-Kutta method. The time of about 3 ms between two maxima of the strain oscillations (period of oscillations) according to equation (12) corresponds to the natural frequency of the real stainless steel exhaust pipe: Ω = 20 kHz. The maximum displacement always occurs in the first oscillation and it is twice as large (dynamic load factor K = 2) in the quasi-static load regime, compared to the strain under static load of the same pipe. This can be regarded as an additional validation of the structural dynamics model used here.

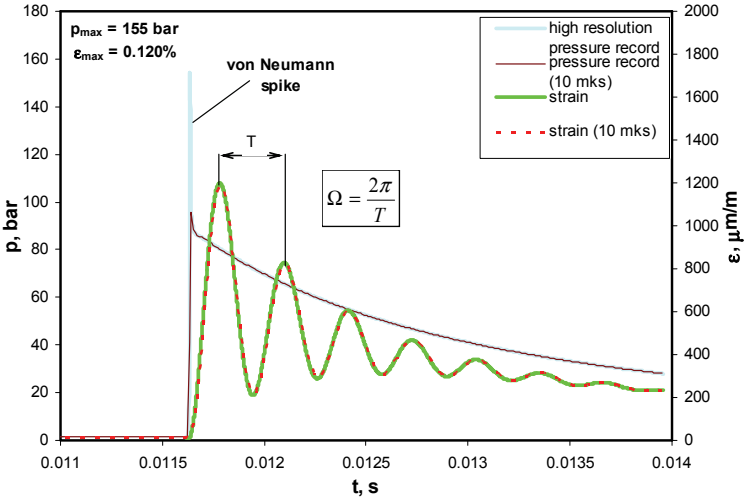

Fig. 10. Calculated mechanical response of exhaust pipe (D = 510 mm, h = 15 mm) under detonation pressure load of a radiolysis gas mixture with 40% nitrogen

5. Results of numerical simulations

With the described 1D computational program the detonation transitions in different radiolysis gas-nitrogen mixtures were simulated. Figure 11 summarizes all accomplished computations, whereby for each nitrogen dilution several values for run-up-distance to the DDT point (x_D) were examined. The white band of realistic run-up-distances to the detonation onset shown in Fig. 11 was estimated using experimental data and our DDT model described previously (Kuznetsov et al., 2002; Kuznetsov et al., 2005). According to this model, the DDT can only occur if the thickness of the turbulent boundary layer in the unburned gas is 10 times higher than the detonation cell size. As Fig. 11 shows, this distance to the DDT point (open blue points) increases exponentially with increasing nitrogen dilution of the radiolysis gas and could reach approx. 8 m for 60% N_2. For 80% N_2 in radiolysis gas the computed distance to the DDT is much larger than the pipe length (L = 12.5 m).

Independent of the realistic range of run-up-distances for nitrogen diluted radiolysis gas mixtures, numerical calculations were performed outside the realistic range to examine the

influence of the run-up distance on the maximum pressure and pipe deformation. Main results of numerical calculations of maximum circumferential pipe strain under radiolysis gas detonation pressure loads are shown in Fig. 11 for all nitrogen dilutions and run-up-distances. Detonations of pure radiolysis gas (0%N_2) and highly nitrogen diluted radiolysis gas (80%N_2), giving low levels of deformations, will not be considered in details. Other calculations resulting in the highest strain will be analyzed in the next sections.

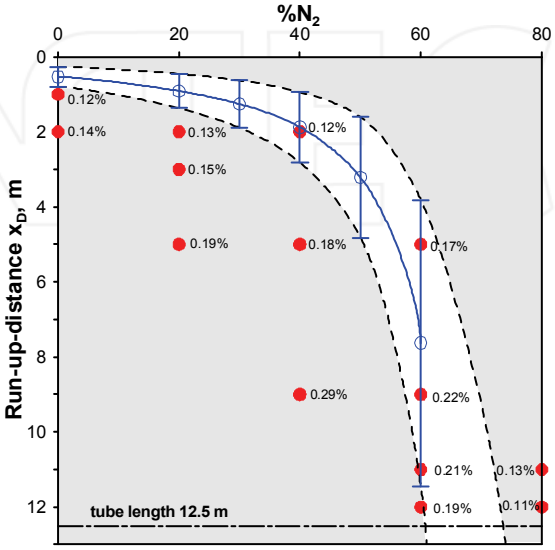

Fig. 11. Overview of the computations: dashed lines indicate upper and lower bounds of run-up-distances to DDT. For every computation the maximum calculated piping strain is indicated (as a label near red point)

5.1 Results for 20% nitrogen

For radiolysis gas - nitrogen mixtures with 20%N_2 three different distances from the ignition to the DDT point were simulated: x_D = 2, 3 and 5 m (see red points in Fig. 11). The ignition of the radiolysis gas took place at x = 0. Figure 12 summarizes the computed pressure-time records (top), plotted at the sensors position (as an x-t - diagram), and peak pressure history (bottom) for the DDT point x_D = 2 m.

Figure 12 (top) shows that DDT occurs 4 ms after the ignition. The blue dotted line corresponds to the position of the accelerating flame front (FF). The upper dotted black line shows the position of the precursor shock wave (SW) which leads to the formation of a pre-compressed and preheated zone ahead of the flame (of up to 1 m length). The strength of the precursor shock wave changes from 4.4 to 7 bar. It results in an overdriven detonation just after the DDT point with a maximum pressure of 110 bar compared to the 48 bar for a steady-state detonation (DW) beyond the pre-compressed zone. The maximum pressure (162 bar) occurs at the tube end due to the detonation reflection. The strength of the reflected wave (RW) decays rather fast from 162 bar to 46 bar over the length of 1.5m.

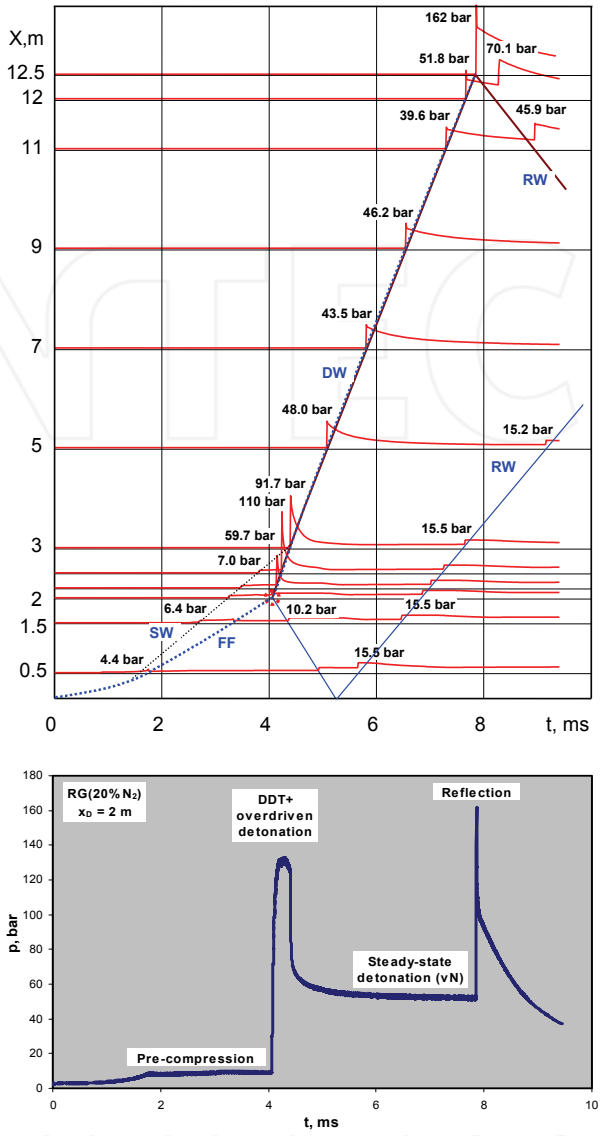

Fig. 12. Computed x-t-diagram (top) and computed peak pressure in the pipe (bottom) for radiolysis gas with 20% nitrogen and a DDT point at $x_D = 2$ m

The maximum pressure history is shown in Fig. 12 (bottom). Four characteristic periods of pressure load can be distinguished from the peak pressure record: (I) pre-compression (P_m = 4.4-7 bar); (II) DDT and overdriven detonation (P_m = 48-110 bar); (III) steady-state detonation ($P_m = P_{vN}$ = 43-48 bar); (IV) detonation reflection (P_m = 162 bar). Each time period can be spatially localized using the x-t-diagram. The first period takes place before the DDT

point x_D= 2 m, the second one extends up to 1 m after the DDT point, period (III) is between x = 3 m and end of the tube at x = 12.5 m, and period (IV) is localized at the tube end x = 12.5 m. The highest pressure corresponds to the DDT and to the reflection at the tube end.

For tube strain, the maximum pressure is not the only important pressure load characteristics. Another important property is the pressure impulse or characteristic pressure loading time. Figure 13 shows the dynamics of the pressure load function for several locations near the DDT point. The closer to the DDT point a pressure sensor is located, the higher is the measured maximum pressure, but the smaller becomes the pressure loading time or pressure impulse.

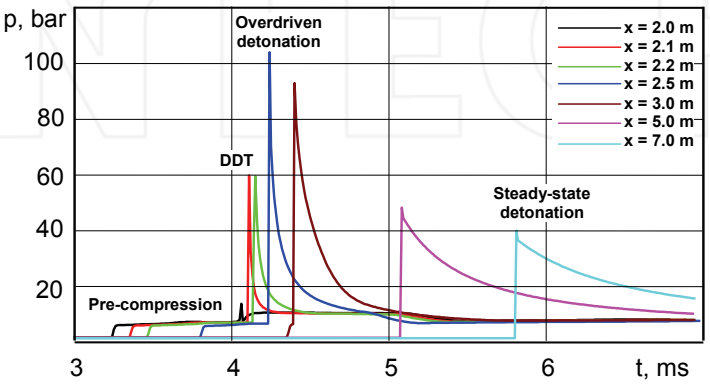

Fig. 13. Pressure load profiles for several locations near the DDT point (x_D=2 m)

The deformations of the modelled tube at different positions have been calculated using a 1D model for the mechanical response of an unconfined cylindrical shell to dynamic pressure loads. To be conservative, the tube dimensions of the weaker part (510x15 mm) were assumed for whole tube. Fig. 14 represents calculated strain signals in form of an x-t-diagram to demonstrate the mechanical piping response to the dynamic pressure load. As Fig. 14 shows, the maximum deformations occur close to the DDT point and at the tube end. However, the maximum pressure impulse was achieved at the distances more than 4 m. The calculated frequency of strain signal oscillations of about 20 kHz is consistent with exhaust pipe dimensions and stainless steel properties.

A comparison of the maximum pressure and maximum strain signal, shown in Fig. 15, demonstrates that the maximum pressure is indeed responsible for the maximum deformation of the pipe. This means that a quasi-static pressure loading regime takes place. Maximum pressure and maximum deformation are located at same positions. In fact, with a natural frequency of the pipe of 20 kHz the characteristic pressure load time has to be more than 2 ms to produce only pressure dependent strain. Generally, maximum deformation does not exceed the critical value for stainless steel ε_m = 0.2%. The computed strain reaches only 0.13% at the tube end.

As it follows from Fig. 15, the highly loaded zones with maximum deformation extend about 2 m after the DDT point and 1.5 m before the tube end. The mechanical response model gives the maximum strain directly at the tube end because the model does not take into account that in reality this part of the tube is much stronger due to the end flange.

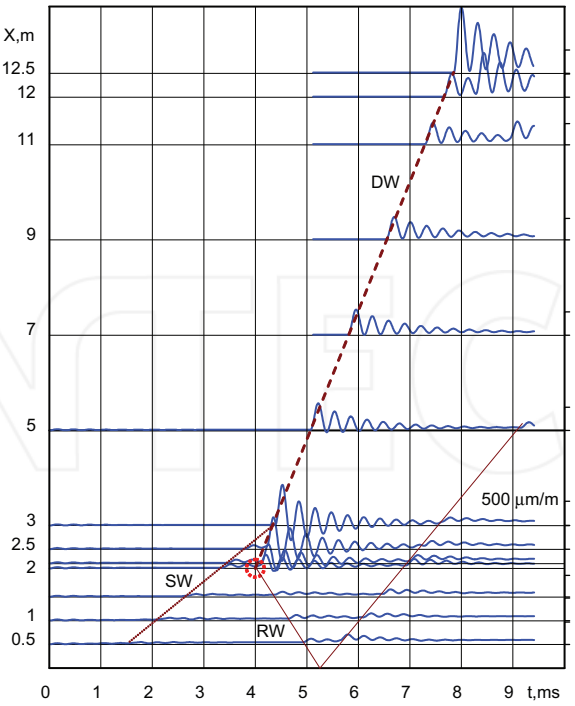

Fig. 14. *X-t* diagram of strain wave propagation under radiolysis gas detonation: scale of a strain signal is shown on the right axis (1 division is 500 µm/m or 0.05%): SW = precursor shock wave; DW = detonation wave; RW = retonation wave

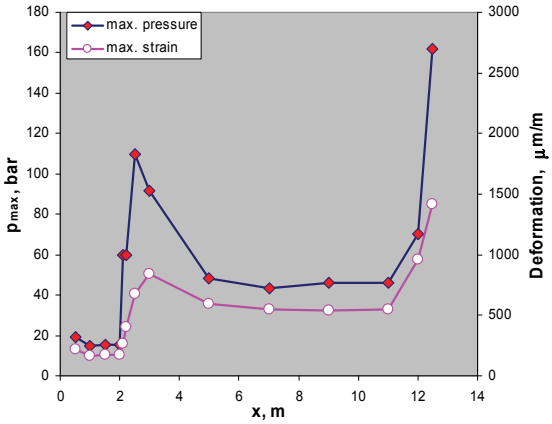

Fig. 15. Maximum pressure load and maximum deformation of the 12.5 m tube under radiolysis gas detonation loads

In the case of a later detonation transition (x_D = 3 m) qualitatively very similar results for calculated pressure load and mechanical response have been obtained. The maximum pipe

strain rises to 0.15% in this case. For a late detonation transition (x_D = 5 m) the computed maximum piping strain is close to the plasticity limit ε_m = 0.19%. But these two cases with late DDT are already far outside of the realistic range of DDT point distances x_D that can be expected for the particular gas mixtures. It can be stated that for a late DDT-position longer pre-compressed zone and longer over-driven detonation zone with higher level of deformations can occur. For instance, the pre-compressed zone extends over 7.5 m for x_D = 5 m, compared to 3 m for x_D = 2 m.

5.2 Results for 40% nitrogen

For radiolysis gas - nitrogen mixtures with 40%N_2 three different distances from ignition to the DDT point were simulated: x_D = 2, 5 and 9 m (see Fig. 11). The ignition of the radiolysis gas took place at x = 0. For the DDT point x_D = 2 m the pre-compressed zone length extends over 4 m from the ignition point. A maximum pressure of about 88 bar for the over-driven detonation and 155 bar for the reflected pressure with a maximum strain of ε_m = 0.12% were obtained for this case. The maximum pressure was lower than in case of 20%N_2 because of less energetic radiolysis gas mixture.

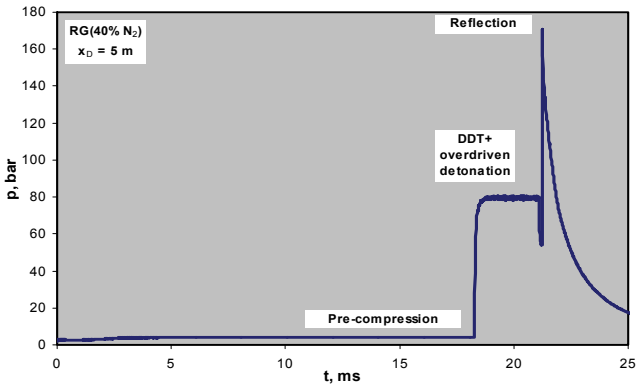

Fig. 16. Computed peak pressure record for radiolysis gas with 40% nitrogen and a DDT point at x_D = 5 m

For the DDT point x_D = 5 m the pre-compressed zone extends practically up to the tube end. A maximum pressure of about 80 bar for over-driven detonation and 170 bar for reflected pressure with a maximum strain of ε_m = 0.19% was observed in this calculation. The peak pressure record (Fig. 16) demonstrates that only an over-driven radiolysis gas detonation without steady-state CJ-detonation occurs in this case. The reflection of the over-driven detonation will be much stronger than the steady-state detonation.

The most dangerous scenario was observed for a late detonation initiation at x_D = 9 m. In this case the precursor shock wave is reflected at the tube end before the detonation onset. Figure 17 shows an *x-t* diagram of the DDT process and simultaneously a peak pressure record for this scenario.

The peak pressure record (Fig. 17, bottom) demonstrates a significant difference of the maximum pressure level compared to all previous cases. First of all, due to the leading precursor shock wave reflection, the radiolysis gas mixture has two times higher initial

pressure prior the detonation (9.2 bar instead of 4.1 bar). This results in two times higher detonation pressure (165 bar instead of 87 bar for overdriven detonation without precursor shock wave reflection) which finally leads to a higher maximum hoop strain of ε_m = 0.16%. Both pressure effects of the reflection and over-driven detonation are superimposed in time with an extremely high resulting pressure of about 300 bar. It produces a very high tube deformation (ε_m = 0.29%) which is higher than the yield limit (ε_m = 0.2%) for stainless steel.

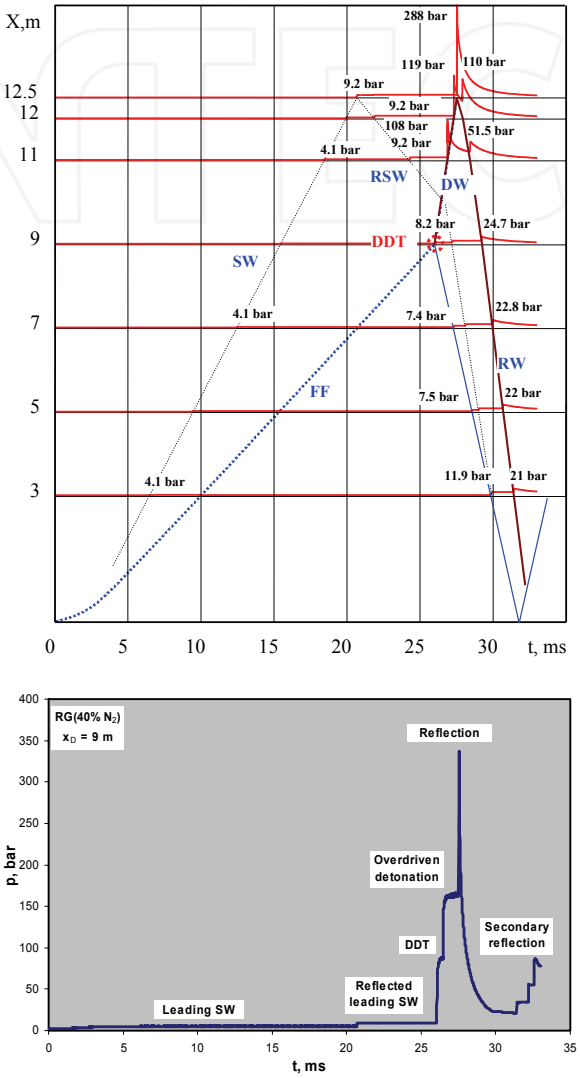

Fig. 17. Computed *x*-*t*-diagram (top) and computed peak pressure record (bottom) for radiolysis gas with 40 vol% nitrogen and a DDT point at x_D = 9 m

5.3 Results for 60% nitrogen

For radiolysis gas - nitrogen mixtures with 60%N_2 four different distances from the ignition to the DDT point were simulated: x_D = 5, 9, 11 and 12 m (Fig. 11). For the DDT point x_D =5 m the pre-compressed zone propagates practically up to the tube end with precursor shock reflection. This is practically the same behavior as for the 40%N_2 radiolysis gas mixture and a distance to the DDT point of x_D = 9 m. The maximum reflected pressure was about 300 bar and the maximum strain was calculated to be ε_m = 0.17%. In the simulations with later detonation onset at x_D = 9, 11 and 12 m, the precursor shock wave was reflected several times at tube ends. In all these cases the maximum pressure achieved at the tube end was approx. 330 – 360 bar. A maximum deformation of ε_m = 0.22% was calculated with a DDT point at x_D = 9 m.

6. Evaluation of maximum deformations

For the computation of the stress and strain of the exhaust pipe a linear oscillator model was used in this work. Here a thin cylindrical piping segment will have a displacement by an elastic oscillation only, axial displacement was neglected. From the FA1D detonation calculations time-dependent internal pressures along the tube were determined for different radiolysis gas mixtures and different DDT points. The following properties were used in the calculations for the stainless steel No. 1.4541: Young modulus of elasticity E = 203000 MPa and density ρ = 8000 kg/m^3.

In the present work we used Hooke's law (or the linear-elastic approach) for the calculations of stress-strain dependence. But in reality Hooke's law is only valid for the portion of the stress-strain curve before the yield limit when material becomes plastic. Another important issue for the computation of piping strain using real stress-strain curves is that material properties depend on the strain rate as well. Our previous experiments with radiolysis gas detonations in stainless steel pipes resulted in strain rates of $\dot{\varepsilon}$ = 100-300 1/s in the elastic and $\dot{\varepsilon}$ = 1000-2000 1/s in the plastic regime of deformation (Kuznetsov et al., 2007b). Appropriate stress-strain curves made by MPA Institute for same stainless steel No. 1.4541 are represented in Fig. 18 (Stadtmüller, 2006). Using zoomed initial part of this strain-strain curve for high strain rate $\dot{\varepsilon}$ = 1000 1/s we can see that even for the highest deformation ε_m = 0.22% inside the realistic range of run-up-distances (see Fig. 11), obtained for 60%N_2 radiolysis gas detonation with a DDT point x_D = 9 m, the tube expands practically in the linear elastic mode (Fig. 19). For the maximum calculated exhaust pipe deformation ε_m = 0.29% outside the realistic range of DDT point we have to take into account plasticity of the material. With the assumption of the same value of the work of deformation W for elastic and plastic regime

$$W = R \cdot S \int_0^{\varepsilon_e} \sigma_{elastic} d\varepsilon = R \cdot S \int_0^{\varepsilon_p} \sigma_{plastic} d\varepsilon = const\,, \tag{20}$$

where R and S are piping radius and cross-section area, we can estimate the maximum plastic deformation corresponding to the calculated value ε_m = 0.29% in an elastic approach. First estimation gives a value ε_m = 0.41% for plastic deformation corresponding to the value ε_m = 0.29% in an elastic approach. This means that even with nonrealistic DDT point taken as a "worst case" the maximum deformation does not exceed 1%.

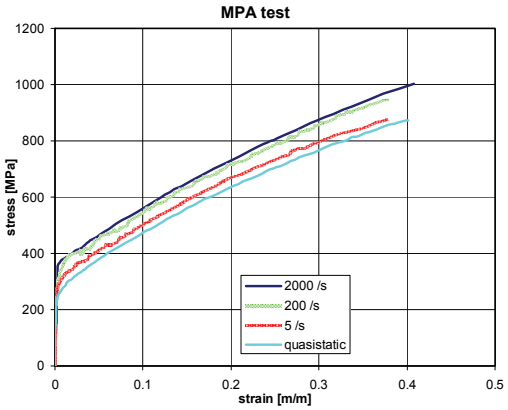

Fig. 18. Dynamic stress-strain characteristics for stainless steel No 1.4541 (Stadtmüller, 2006)

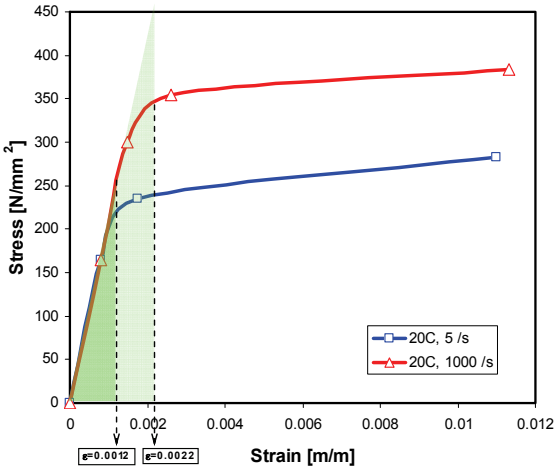

Fig. 19. Mechanical response of the exhaust pipe for dynamic detonation pressure load with a quasi-static ($\dot{\varepsilon}$ = 5/s) and dynamic strain rate ($\dot{\varepsilon}$ = 1000/s)

7. Experimental verification of FA1D-code

Experiments on radiolysis gas detonation have been performed in a tube designed similar to a typical BWR exhaust tube. The tube was fabricated of austenitic stainless steel DIN 1.4541 with following material properties: Young modulus of elasticity E = 203000 MPa and density ρ = 8000 kg/m3. The tube was installed into a safety vessel with 80 mm wall thickness, certified for a static pressure of 100 bar. The tube with a length of 12.25 m consisted of two parts that were 4275 and 7501 mm long with different outer diameters and wall thicknesses: (I) 419x20 mm and (II) 510x15 mm. Both parts of the tube were connected via a conic part of 300 mm length and 20 mm wall thickness. Total weight of the piping structure with the flanges was approx. 3500 kg.

Stoichiometric hydrogen-oxygen mixtures diluted with 0 to 55% nitrogen at an initial pressure of 1.6 bar and a temperature of about 30 ^{O}C have been used in order to define initial conditions leading to the strongest detonation pressure and the maximum tube deformation. Several tests have been carried out at reduced initial pressures of 0.4 and 0.8 bar prior the main experimental series. Before each test the tube was evacuated up to a pressure of less than 0.1 mbar. After the evacuation the test mixture was injected into the test tube up to required initial pressure. The concentration of each mixture component was controlled via mass flow rates. The mixture quality was additionally checked by a gas analyzer connected via bypass line. The test mixture was ignited by a spark plug, mounted axially in the flange at the stronger part of the tube to reproduce the most conservative scenario where the maximum detonation pressure appears in the weakest part of the tube.

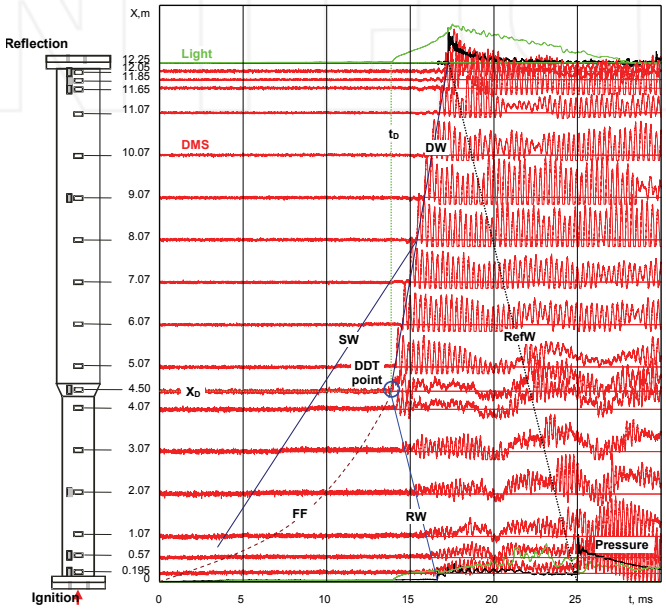

Fig. 20. *X-t* diagram of detonation process based on records of strain gauges (red lines), pressure sensors (black) and photodiodes(green): SW = precursor shock wave; FF = flame front; DW = detonation wave; RW = retonation wave; RefW = reflected detonation wave

A schematic of the tube and the gauges location is shown in Fig. 20. To record the radiolysis gas detonation pressure and dynamics of the flame propagation 4 pressure sensors and 2 photodiodes as light sensors were installed in both end flanges. The axial position of light sensors allows registering the DDT moment due to its very intensive light signal of the local explosion. 17 circumferential and 8 longitudinal DMS strain gauges with temperature compensation were fixed on the cylindrical surface of the tube to measure the tube deformations and the arrival time of the shock waves and the detonation wave.

Figure 20 demonstrates an example of *x-t* diagram of detonation process of radiolysis gas mixture with 40% nitrogen at 1.6 bar initial pressure. The diagram represents signal records in time for different sensors locations along the test tube. When shock wave or detonation wave arrives at a sensor position it causes a sharp increase of the signal. For instance, by

using the points with sharp pressure or strain increase as arrival time, the well pronounced trajectories of the precursor shock wave (SW), detonation wave (DW), reflected detonation wave (RefW), and retonation wave(RW) were identified on the *x*-*t* diagram (Fig. 20). Due to the precursor shock wave with a pressure of 3.5 bar and a velocity of 600 m/s, generated by an accelerating flame front (FF), an overdriven detonation takes place in the pre-compressed radiolysis gas mixture with an initial pressure of 3.5 bar. The subsequent detonation reflection from the end flange results in a significant increase of the detonation pressure with propagation of reflected detonation wave in opposite direction.

The experiments showed that with increasing nitrogen dilution, the DDT point shifts towards the tube end with production of extremely high pressure and piping deformation as result of the cumulative effects of pre-compression, reflection and local explosion during the DDT process.

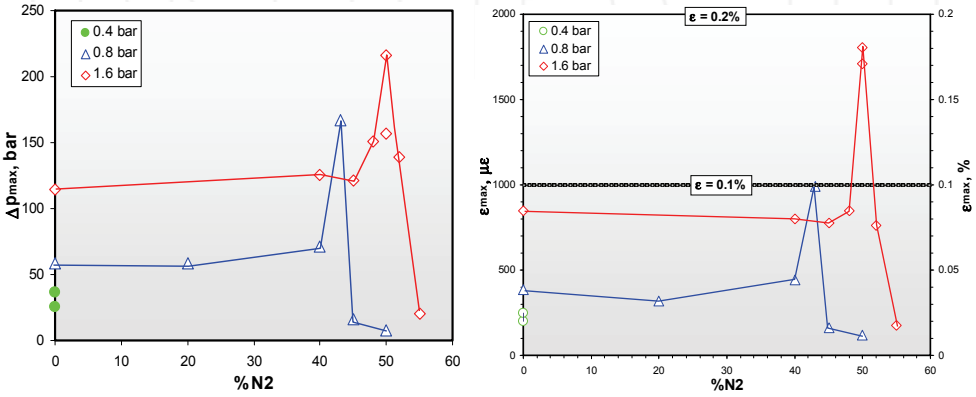

Fig. 21. Maximum experimental pressure load (left) and maximum measured hoop strain (right) along the tube vs. nitrogen dilution for different initial pressures (yield limits of 0.1% and 0.2% are shown)

Finally, all the experimental data on maximum pressure and maximum strain along the tube are summarized in Figs. 21 as a function of nitrogen dilution of radiolysis gas mixture. The experimental data for maximum hoop strain along the tested tube show that deformation of the pipe is consistent with level of pressure load. As it follows from these plots, the maximum pressure load and the maximum tube deformations occurred for nitrogen dilution of 50% at an initial pressure of 1.6 bar when a scenario with late detonation initiation was realized. This means that higher nitrogen dilution leads to the actually worst case scenario, in which the maximum tube deformation achieves a value of 0.17-0.18%, or practically two times higher than a scenario with detonation of pure radiolysis gas (0%N_2) proposed in our previous work (Kuznetsov et al., 2007). Such level of experimental hoop strain is consistent with calculated deformations in the range of 0.19-0.22%, obtained for "late DDT" scenarios with run-up distances of 9-12 m from the ignition point (see Fig. 11). The lower experimental maximum strain can be explained due to the reinforcing effect of the end flange, which makes the cylindrical tube wall stronger, compared to the model of an unconfined cylindrical shell, assumed in the numerical calculations.

Generally, maximum tube deformations of 0.17-0.18% from radiolysis gas detonations are less than the yield limit of 0.2% for austenitic stainless steel. This means that the BWR

exhaust tube remains intact even in the worst case scenario of radiolysis gas detonation. Additionally, we have to point out that in case of combustion (no detonation initiation at nitrogen concentration more than 52 vol. $\%N_2$), as it follows from Fig. 21 (right), the maximum deformation is 10 times smaller than in case of the radiolysis gas detonation. This means that stoichiometric hydrogen-air mixture with $56\%N_2$ if it would be ignited from end flange in such a smooth and large (~0.5 m i.d.) tube without obstacles would not detonate. As it follows from the papers (Kuznetsov et al., 2005; Liberman et al., 2009), reduction of the tube diameter will shorten the run-up distance to detonation. This may be sufficient to initiate detonations in less reactive mixtures than in our tests. Decreasing of initial pressure reduces the mixture detonability and detonability limit shifts to lower nitrogen concentration as well.

8. Conclusions

To describe the deflagration-to-detonation transition (DDT) of radiolysis gas mixtures diluted with nitrogen and/or steam the new 1-dimensional computational code FA1D was developed and experimentally verified. The program allows performing a continuous mechanistic analysis of the complex processes with deflagration-to-detonation transition in closed pipes leading to the highest internal pressure loads.

For radiolysis gas mixtures with nitrogen dilution from 0 to 80% different DDT run-up-distances were postulated and resulting pressure loads and maximum deformations of an exhaust pipe with 510-mm o.d. and 15-mm wall thickness were calculated. The real "worst case" with a maximum pressure load and deformation always arose at the tube end as a result of a cumulative effect of precursor shock reflection, DDT and detonation reflection processes (so called "late detonation").

With a simplified linear-elastic model of piping response to dynamic pressure loads the results of the calculations were very close to the experimental data. The obtained calculated maximum strains are quite low and present no danger for the integrity of the exhaust pipe fabricated from the material DIN 1.4541. Nitrogen dilution of the radiolysis gas does not reduce the stress of the pipe. On the contrary, up to some critical nitrogen concentration it has a promoting effect on stress of the tube by producing "late detonation".

The real scale experiments with a BWR exhaust pipe showed that the detonation of nitrogen diluted radiolysis gas mixtures leads to significantly larger and safety-relevant piping deformation compared to pure radiolysis gas. Maximum pressure loads with maximum deformations occur just after the DDT point and near the reflection end. It was shown that even the real "worst-case" scenario of radiolysis gas detonation with the critical nitrogen dilution ($50\%N_2$) would not lead to a structural damage of the exhaust pipe.

9. Acknowledgments

We are very grateful to Mr. T. Franke and EnBW Kernkraft GmbH, Philippsburg, Germany for funding and technical support of this work.

10. References

Baker, W.E., Cox, P.A., Westine, P.S., Kulesz, J.J., Strehlow, R.A. (1983) *Explosion Hazards and Evaluation*, Elsevier Publ. Co., 277p.

Bradley, D. (1992) How Fast Can We Burn? *24th Symposium (Int.) on Combustion*, pp. 247-262.

Goodwin, D. G. (2001) *Cantera User's Guide*, California Institute of Technology, Pasadena, CA, USA

Kuznetsov, M.; Alekseev, V.; Matsukov, I. & Dorofeev, S. (2002), Experiments on Flame Acceleration and DDT in Smooth Tubes with Radiolysis Gas for BWR Safety Applications, *Report Vargos Co. for FZK*, December 2002, Saint-Petersburg.

Kuznetsov, M., Alekseev, V., Matsukov, I., Dorofeev, S. (2005) DDT in a Smooth Tube Filled with Hydrogen-Oxygen Mixtures, *Shock Waves*, 14(3), pp. 205 - 215.

Kuznetsov, M.; Redlinger, R. & Breitung, W. (2007a) Evaluation of the Maximum Reaction Pressure from Radiolysis Gas Explosion in Pipes and the Corresponding Pipe Response, *Proc. Annual Meeting on Nuclear Technology*, pp. 211-216, German Nuclear Society, Karlsruhe, Germany.

Kuznetsov, M.; Grune, J.; Redlinger, R.; Breitung, W.; Sato, K.; Inagaki, T. & Ichikawa, N. (2007b) Plastic Deformation and Tube Rupture under Radiolytic Gas Detonation Loads, *Proc. ICONE15*, ICONE15-10377, pp. 1-12, Nagoya, Japan.

Liberman, M.; Kuznetsov, M.; Ivanov, A. & Matsukov, I. (2009) Formation of the preheated zone ahead of a propagating flame and the mechanism underlying the deflagration-to-detonation transition, *Physics Letters A*, 373(5) pp. 501-510.

Lutz, A. E. (1988) A Numerical Study of Thermal Ignition, *Sandia Report SAND88-8228*

Nakagami, M. (2002) Pipe rupture incident of Hamaoka Nuclear power station Unit-1, *Report Chubu Electric Power Co., Inc.*, Japan.

Schröder, V. & Hieronymus, H. (2006) Sicherheits-technisches Gutachten zu möglichen Explosionsdrücken im RA Druckentlastungssystem bei Radiolysegasreaktionen, *Bericht BAM*, März 2006, Berlin, Germany.

Stadtmüller, W. (2006) MPA Stuttgart, Halbjahresbericht 2006-1, GRS-Förderkennzeichen 150, 1297, http://grs-jsri.de

Schulz, H.; A. Voswinkel, & H. Reck (2002) Insights and Lessons Learned from the Brunsbuettel Piping Failure Event, *EUROSAFE Rep.*, GRS/IRSN, Forum for nuclear safety, Berlin

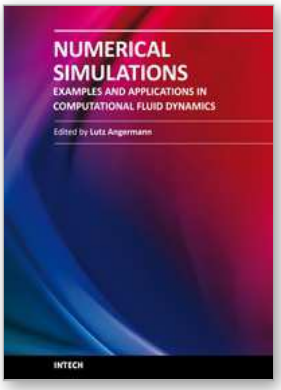

Numerical Simulations - Examples and Applications in Computational Fluid Dynamics

Edited by Prof. Lutz Angermann

ISBN 978-953-307-153-4
Hard cover, 440 pages
Publisher InTech
Published online 30, November, 2010
Published in print edition November, 2010

This book will interest researchers, scientists, engineers and graduate students in many disciplines, who make use of mathematical modeling and computer simulation. Although it represents only a small sample of the research activity on numerical simulations, the book will certainly serve as a valuable tool for researchers interested in getting involved in this multidisciplinary ï¬eld. It will be useful to encourage further experimental and theoretical researches in the above mentioned areas of numerical simulation.

How to reference

In order to correctly reference this scholarly work, feel free to copy and paste the following:

Mike Kuznetsov, Alexander Lelyakin and Wolfgang Breitung (2010). Numerical Simulation of Radiolysis Gas Detonations in a BWR Exhaust Pipe and Mechanical Response of the Piping to the Detonation Pressure Loads, Numerical Simulations - Examples and Applications in Computational Fluid Dynamics, Prof. Lutz Angermann (Ed.), ISBN: 978-953-307-153-4, InTech, Available from: http://www.intechopen.com/books/numerical-simulations-examples-and-applications-in-computational-fluid-dynamics/numerical-simulation-of-radiolysis-gas-detonations-in-a-bwr-exhaust-pipe-and-mechanical-response-of-

INTECH
open science | open minds

InTech Europe
University Campus STeP Ri
Slavka Krautzeka 83/A
51000 Rijeka, Croatia
Phone: +385 (51) 770 447
Fax: +385 (51) 686 166
www.intechopen.com

InTech China
Unit 405, Office Block, Hotel Equatorial Shanghai
No.65, Yan An Road (West), Shanghai, 200040, China
中国上海市延安西路65号上海国际贵都大饭店办公楼405单元
Phone: +86-21-62489820
Fax: +86-21-62489821